Rationalizing polymer swelling and collapse under repulsive to highly attractive cosolvent conditions

Anja Muzdalo, Jan Heyda, and Joachim Dzubiella
Soft Matter and Functional Materials, Helmholtz-Zentrum Berlin, Hahn-Meitner Platz 1, 14109 Berlin, Germany and
*Department of Physics, Humboldt-University Berlin, Newtonstr. 15, 12489 Berlin, Germany**

The collapse and swelling behavior of a generic homopolymer is studied using implicit-solvent, explicit-cosolvent Langevin dynamics computer simulations for varying interaction strengths. The systematic investigation reveals that polymer swelling is maximal if both monomer-monomer and monomer-cosolute interactions are weakly attractive. In the most swollen state the cosolute density inside the coil is remarkably bulk-like and homogenous. Highly attractive monomer-cosolute interactions, however, are found to induce a collapse of the chain which, in contrast to the collapsed case induced by purely repulsive cosolvents, exhibits a considerably enhanced cosolute density within the globule. Thus, collapsed states, although appearing similar on a first glance, may result from very different mechanisms with distinct final structural and thermodynamics properties. Two theoretical models, one based on an effective one-component description where the cosolutes have been integrated out, and a fully two-component Flory – de Gennes like model, support the simulation findings above and serve for interpretation. In particular, the picture is supported that collapse in highly attractive cosolvents is driven by crosslinking-like bridging effects, while the ratio of attraction width to cosolute size plays a critical role behind this mechanism. Only if polymer-cosolute interactions are not too short-ranged swelling effects should be observable. Our findings may be important for the interpretation of the effects of cosolutes on polymer and protein conformational structure, in particular for highly attractive interaction combinations, such as provided by urea, GdmCl, NaI, or $NaClO_4$ near peptide-like moieties.

I. INTRODUCTION

Single polymer coils in solution swell in good solvents and collapse in bad solvents.[1] In a good solvent the effective interaction between polymer monomers is repulsive which tends to swell the polymer. In a bad solvent the interaction is essentially attractive and the coil shrinks until hindered by steric packing effects. On the simplest theoretical level these trends can be qualified by effectively one-component mean-field treatments as pioneered by Flory and de Gennes.[1,2] Here the system free energy $F(R)$ in dependence of coil size R is typically written as[2,3]

$$F(R) \sim R^2/Nb^2 + B_2N^2/R^3 + B_3N^3/R^6, \qquad (1)$$

where the first term is the elastic energy of an ideal chain with N monomers and segment length b, and the other terms account for mutual monomer interactions globally expressed by an virial expansion up to second order in density $\sim N/R^3$. The virial coefficients have to be considered as based on *effective* pair potentials because the (co)solvent degrees of freedom have been integrated out. Scaling law predictions from (1) are basis for the discussion of collapse and swelling in polymer science.[2,3]

The problem of such a perspective is that the information about the detailed effects of solvent or cosolvents are lost. In the recent years, however, the complexity and resolution of experimental investigations has increased, and there is growing interest about how the specific binding mechanisms of cosolutes may alter global polymeric properties, such as the coil-globule transition.[4] A particularly important example is the specific effect of cosolutes, such as ions, osmolytes, or denaturants on protein structure and stability.[5–15] Here, general polymer principles are typically employed as a starting point for the investigation of those cosolute effects.[16,17] In this spirit, relatively simple thermosensitive polymers such as the poly(N-isopropylacrylamide) (PNIPAM) homopolymer often serve as a experimental peptide model.[18,19] On the computational side, simulations allow to address fundamental questions in the framework of polymer physics, such as swelling and collapse of idealized, purely hydrophobic homopolymer in denaturants, osmolytes, or salts,[20–23] or more generic polymer-cosolute systems.[24–26]

An important experimental reference to our study are the works by the Cremer group on (methylated) urea and ion-specific effects on the lower critical solution temperature (LCST) of PNIPAM[18,19] and the relatively simple, elastin-like peptides.[19,27] The qualitative change in the LCST, $\Delta T(\rho)$, with cosolute concentration ρ can be used as an index whether polymer coils swell or collapse with the addition of cosolutes.[9] For instance, PNIPAM swells in methylated urea, while it collapses with the addition of nonmethylated urea. In contrast, the relatively hydrophobic elastin-like peptides swell in urea, consistent with computer simulations of simple homopolymers.[20–23] For both PNIPAM and elastin peptides, both being electroneutral, collapse and swelling in salt strongly depends on salt type. Hence, there is a wide variety of observed behaviors which are challenging to categorize.

Typically polymer collapse (or protein stabilization) is argued to originate from the preferential exclusion of repulsively interacting cosolutes, thereby trying to mini-

mize cosolute-accessible surface area.[7,10,11,28] Sagle *et al.*, however, argue that urea collapses PNIPAM due to a direct binding mechanism featuring strong, short-ranged attractions provided by multivalent hydrogen bonds.[19] Crosslinking then leads to shrinking of the coil. This were not the case, they say, for methylated urea, or urea interacting with peptides, where interactions are only monovalent and very weakly attractive. Hence, specific values of binding parameters such as attraction strength and width are probably decisive whether a given polymer swells or not.

The crosslinking effect may also be important for other cosolutes or salts, such as $NaClO_4$. Its effects on the LCST of PNIPAM does not conform with the usual Hofmeister series.[9,18] On the other hand, it is known to strongly interact with the peptide group.[18,19] Indeed recent explicit-water computer simulations together with circular dichroism (CD) and Förster resonance energy transfer (FRET) measurements on $NaClO_4$-destabilized α-helical peptides demonstrated highly compact, disordered states crosslinked by a network of sodium and perchlorate ions.[29] Thus, collapsed states, although appearing similar on a first glance, may result from very different mechanisms with quite distinct final structural and thermodynamics properties. Indications of the latter stem from the experimental characterization of $NaClO_4$ denatured molten globules[5,29,30], which may be cosolute rich, with implications in protein folding.[31,32] We note that similar considerations may be important in the ion-induced collapse of polyelectrolytes by ion condensation beyond simple Debye-Hückel electrostatics.[33–36] Hence, finding minimalistic models which can describe this vast variety of effects are in need.

The aim of this paper is to theoretically investigate polymer collapse and swelling under the action of cosolutes on a highly generic level. For that we first start to employ implicit-solvent computer simulations of a Gaussian polymer chain including explicit cosolutes, and we systematically vary monomer-monomer and monomer-cosolute attraction strengths. Our polymer model is similar to that of Toan *et al.*[37] who systematically investigated polymer swelling and collapse (with consequences to conformational kinetics) in dependence of monomer-monomer attraction strength in purely implicit solvent. Our simulations indicate chain collapse for highly attractive cosolute conditions as also found in recent on- and off-lattice computer simulations by Antypov and Elliot.[26] The results from the simulations are then rationalized by two theoretical models: First, an effective interaction model where the action of the monomer-cosolute is explicitly integrated out in a statistical mechanics framework.[38] The results are then discussed on a one-component level as in eq (1). Secondly, we extend the Flory-deGennes description in eq. (1) to a full 2-component description and calculate swelling behavior in dependence of interaction strengths and cosolute density. Both theoretical descriptions qualitatively agree with the simulations giving important rational. Importantly, all three approaches point to polymer collapse at highly attractive cosolute conditions due to crosslinking-like bridging effects as argued by Sagle *et al.*[19]

II. POLYMER-COSOLUTE LANGEVIN COMPUTER SIMULATION

A. Model and Methods

In our simulation we consider a single, coarse-grained homopolymer with $N = 100$ connected monomers in an implicit solvent background in a volume V. In addition, N_c explicit cosolutes with mean number density $\rho_c^0 = N_c/V$ are added to the system. All particles, polymer monomers and cosolutes, are interacting via the Lennard-Jones (LJ) pair potential

$$V_{ij}(r) = 4\epsilon_{ij}[(\sigma_{ij}/r)^{12} - (\sigma_{ij}/r)^6], \tag{2}$$

where $i = m, c$ stands for monomer or cosolute atom, respectively. The value of the size $\sigma_{ij} \equiv \sigma = 0.3385$ nm is chosen to be be fixed for all interactions in our simulations. It is the same value as in Toan *et al.*'s work[37] and is comparable to the typical size of the methyl group. The interaction energy ϵ_{ij} will be systematically varied as described below. The polymer is modeled by a Gaussian chain with harmonic nearest-neighbor bond interactions $V_{\mathrm{bond},ij} = 0.5k(\mathbf{r}_i - \mathbf{r}_j)^2$ and a spring constant $k = 320$ kJ mol^{-1} nm^{-2}. The latter is chosen such that we end up with the same effective Kuhn length $b = 0.38$ nm for the ideal polymer as in Toan *et al.*'s work.[37] The mean end-to-end distance in the ideal case is thus $\bar{R} = \sqrt{N}b = 3.8$ nm. The corresponding ideal radius of gyration $R_g^0 = 1.55$ nm. The LJ interaction between a monomer and its next two nearest neighbors is excluded.

The polymer-cosolute system is simulated in the NVT-ensemble using stochastic computer simulations. Every atom is propagated via the Langevin equation

$$m\ddot{\mathbf{r}}_i + m\xi\dot{\mathbf{r}}_i = \sum_j \mathbf{F}_{ij} + \mathbf{F}^{(R)}, \tag{3}$$

where $\mathbf{r}_i$ is the position of a particle i, $m = 8$ amu its (irrelevant) mass, $\xi = 0.5$ ps^{-1} is the friction constant, $\mathbf{F}_{ij}$ the force between particles i and j, and $\mathbf{F}^{(R)}$ the stochastic force stemming from the solvent kicks. The stochastic force has zero mean $\langle \mathbf{F}^{(R)} \rangle = 0$ and fluctuation-dissipation is obeyed via $\langle \mathbf{F}_i^{(R)}(t)\mathbf{F}_j^{(R)}(t') \rangle = 2k_BT\xi\delta_{ij}\delta(t-t')$. The simulations are performed using the Gromacs simulation package[39] with periodic boundary conditions, an integration time step of 4 fs, and lincs bond constraints. The simulation box is cubic and has a box length of 13 nm. We fix the mean cosolute density $\rho_c^0 = 3$ nm^{-3} ($\simeq 5$ mol/l) chosen to represent a typical denaturant density. With that we end up with $N_c = 6591$ cosolutes in the simulation. We simulate every system for at least 1 μs.

If the polymer is in a swollen or collapsed state can be judged by inspection of the radius of gyration R_g scaled by the one of the ideal polymer R_g^0. If $R_g/R_g^0 > 1$ the polymer is swollen, if $R_g/R_g^0 < 1$, it is collapsed. The statistical error of R_g in our simulations is estimated by block averages: the trajectory is divided into n blocks of the same length (at least 200ns, but up to 1μs) and the standard deviation of these block averages with respect to the mean was calculated and divided by $\sqrt{n}$ to obtain the error.

Whether the LJ interaction $V_{ij}(r)$ is globally attractive or repulsive can be quantified by the second virial coefficient defined via

$$B_2^{ij} = -\frac{1}{2}\int \mathrm{d}^3 r \left[\exp(-\beta V_{ij}(r)) - 1\right], \qquad (4)$$

where $\beta = (k_B T)^{-1}$ is the inverse thermal energy and we use $k_B T = 1$ as the energy scale in the following. For the LJ potential, the B_2 in dependence of the LJ interaction energy ϵ is shown in Fig. 1: for interaction values $\epsilon \lesssim 0.3$, the B_2 is larger zero since excluded volume contributions from distances $r < \sigma$ dominate. At $\epsilon = 0.3$ the B_2 vanishes, i.e., interactions are ideal on a 2-body level. For $\epsilon \gtrsim 0.3$ effectively the interactions are attractive. In the polymer-only case (no cosolutes), those regimes can be identified with the usual good solvent regime (swelling), Θ-solvent (ideal), and bad solvent (collapse), respectively.[3] Indeed previous simulations showed a collapse transition of the 100mer in the weakly attractive regime with ϵ around 0.4. For $\epsilon \gtrsim 0.6$ the chain collapses in dense, compact states. This regime was characterized as highly attractive.[37]

In our simulations we vary systematically both ϵ_{mm} and ϵ_{mc} between 0 and 1, thereby studying the whole range of repulsion to strong attraction for both components, that is, monomer-monomer and monomer-cosolute interactions. For simplicity the cosolute-cosolute interaction will be fixed to $\epsilon_{cc} = 0.3$ mimicking a near-ideal cosolute solution. Nonideality may also influence polymer swelling and shrinking behavior due to osmotic effects but these effects are out of scope of this paper.

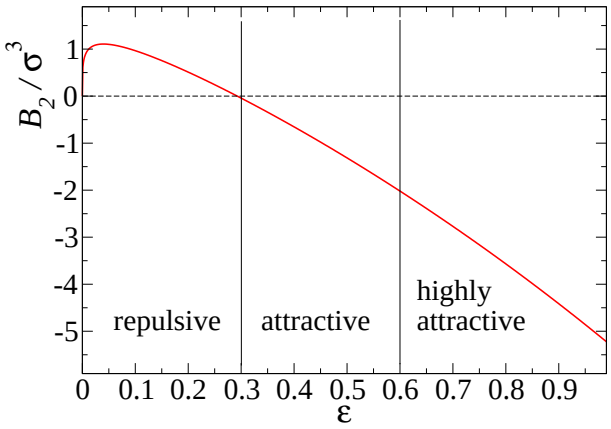

FIG. 1: Second virial coefficient eq. (4) of the Lennard-Jones interaction eq. (2) versus LJ interaction energy ϵ. The B_2 value can be used to classify the interaction into mainly 'repulsive' ($B_2 > 0$), 'attractive' ($B_2 < 0$), and 'highly attractive' ($B_2/\sigma^3 \lesssim 2$).

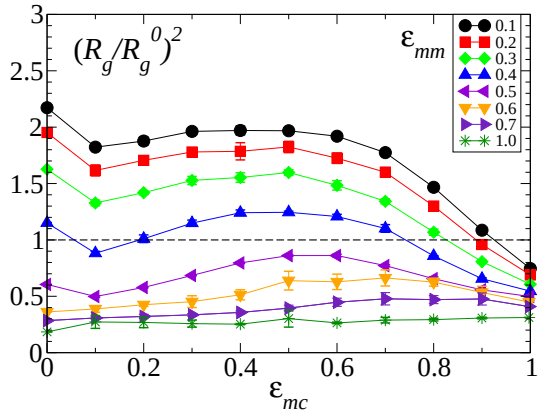

FIG. 2: The squared radius of gyration R_g^2 of the polymer scaled by the ideal value $(R_g^0)^2$ versus the monomer-cosolute interaction strength ϵ_{mc} for varying monomer-monomer interaction ϵ_{mm}. If $(R_g/R_g^0)^2 > 1$ the polymer is swollen, if $(R_g/R_g^0)^2 < 1$, it is collapsed. Error bars are typically of symbol size.

B. Simulation Results

In Fig. 2 we plot the size of the polymer expressed by the radius of squared gyration R_g^2 versus monomer-cosolute attraction ϵ_{mc} for varying monomer-cosolute attraction ϵ_{mm}. Note that R_g^2 is scaled by $(R_g^0)^2$, the size of the ideal polymer, to easily distinguish between swollen ($R_g/R_g^0 > 1$) and collapsed ($R_g/R_g^0 < 1$) states. Let us first focus on vanishing $\epsilon_{mc} = 0$, i.e., the polymer-only case: the polymer is swollen in a good solvent $\epsilon_{mm} \lesssim 0.3$, almost ideal for $\epsilon_{mm} = 0.4$, and collapsed for $\epsilon_{mm} \gtrsim 0.5$.

If now the cosolutes are 'switched-on' ($\epsilon_{mc} > 0$) to a value of $\epsilon_{mc} = 0.1$, where monomer-cosolute interactions are repulsive (cf. Fig. 1), the chain shrinks considerably for $\epsilon_{mm} < 0.6$. This is expected since the exclusion of repulsive monomers from the polymer region is entropically disfavored and leads to chain shrinking. For larger $\epsilon_{mm} > 0.6$ the effects are small. For an increased $\epsilon_{mc} = 0.2$ the polymer swells for all of the values of ϵ_{mm}. Hence, the solvent quality overall improves with less monomer-cosolute repulsion (cf. Fig. 1). For very strong monomer-monomer attractions, $\epsilon_{mm} > 0.6$, the effect is quite small and the polymer stays essentially in the collapsed state.

For further increasing $\epsilon_{mc} \gtrsim 0.3$, roughly where monomer-cosolute repulsion turns into attraction, the

swelling of the polymer continues for all ϵ_{mm} to a maximum value R_g^{max} whose corresponding ϵ_{mc}^{max} value depends on ϵ_{mm}. For larger monomer-monomer attraction ϵ_{mc}^{max} is shifted to larger values. For values larger than ϵ_{mc}^{max} the chain collapses again, i.e., there is a reentrant collapse transition for an increasingly attractive monomer-cosolute interaction. This continuous crossover from a good solvent to a bad one with increasing attraction has been observed already in a previous simulations.[26] For not highly attractive intrapolymer interactions $\epsilon_{mm} < 0.6$ and highly attractive polymer-cosolute interactions $\epsilon_{mc} > 0.6$, the chain can be even more strongly collapsed than in the case of highly repulsive monomer-cosolute ($\epsilon_{mc} = 0.1$) interactions. Hence, this regime shows strong compaction by a highly attractive cosolute.

The cosolute-induced effect is strongest for $\epsilon_{mm} \simeq 0.4$, that is, in the ideal to weakly attractive polymer regime. Overall the polymer crosses from collapsed ($\epsilon_{mc} \simeq 0.1$) to swollen ($\epsilon_{mc} \simeq 0.3 - 0.8$) to again collapsed ($\epsilon_{mc} \gtrsim 0.8$) states with the most dominant changes when compared to the other monomer-monomer interactions. Simulation snapshots of the polymer-cosolute system for $\epsilon_{mm} \simeq 0.4$ and ϵ_{mc} =0.1 (collapsed), 0.5 (swollen), and 1.0 (collapsed) are shown in Fig. 3. Note the considerably different amount of cosolutes in the vicinity of the two collapsed states (a) and (c).

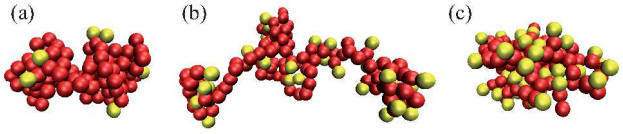

FIG. 3: Simulation snapshots of the polymer-cosolute system for $\epsilon_{mm} \simeq 0.4$ and (a) ϵ_{mc} =0.1 (collapsed), (b) 0.5 (swollen), and (c) 1.0 (collapsed). Cosolutes (yellow spheres) are shown which are found in a cut-off distance of $\sigma 2^{1/6} = 3.8$Å to the polymer backbone (connected red spheres).

To further characterize structural details in the regimes described above we plot the radial one-particle density distributions of the monomers and cosolutes $\rho_m(r)$ and $\rho_c(r)$ in Fig. 4. With r we denote the radial distance to the center-of-mass of the polymer chain. The profiles are plotted for a fixed $\epsilon_{mm} = 0.4$ and varying $\epsilon_{mc} = 0.1$, 0.5, and 1.0. In the collapsed states the polymer density profiles are similar. However, the cosolutes are strongly depleted in the repulsive case, ϵ_{mc} =0.1, while their presence is massively enhanced in the highly attractive case with ϵ_{mc} =1.0. At the most swollen polymer state for $\epsilon_{mc} = 0.5$ the cosolute density is remarkably homogeneous and bulk-like.

III. EFFECTIVE INTERACTION MODEL

In this section we attempt to rationalize some of the swelling and collapse trends we found above in the per-

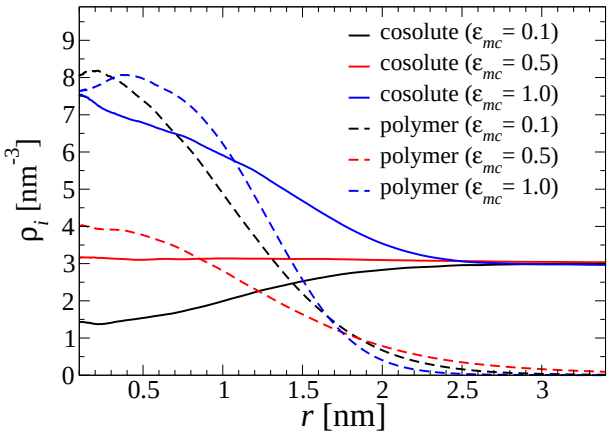

FIG. 4: Radial density profiles $\rho_i(r)$ of polymer monomers ($i = m$) and cosolutes ($i = c$) around the center-of-mass of the polymer. Interaction values are $\epsilon_{mm} = 0.4$ and $\epsilon_{mc} = 0.1$, 0.5, and 1.0 (see legend) corresponding to the snapshots in Fig. 3.

spective of an effective one-component model. For this the effects of the cosolutes have to be integrated out to derive an effective cosolute-induced interaction between two monomers. This is reflected then in an effective B_2 coefficient as used in the one-component Flory approach eq (1). For simplicity we will model the monomers as planar plates and aim only at qualitative statements. We borrow thereby from a similar model introduced within the framework of mesosurface attraction induced by adhesive particles.[38]

Consider two planar surfaces (monomers) with area A in a surface-to-surface distance d in contact with a reservoir of cosolutes at concentration ρ_c^0. The cosolutes interact with the surface with the generic potential $V(z)$ as shown in Fig. 5: the cosolutes are hard spheres with a diameter σ and have an additional attractive (adsorption) energy of strength $\epsilon \leq 0$ and not too large width $\delta \lesssim \sigma/2$. Now consider three situations 1)-3) as also depicted in Fig. 5. In situation 1) the plate distance is $d < \sigma$, i.e, no cosolutes fit between them. This situation can be coined 'depletion' situation. In situation 2), $d > 2\sigma$, and cosolutes can solvate both of the surfaces. In situation 3), $d \simeq \sigma$, one bound particle can interact with the two surfaces simultaneously. This situation can be named 'bridging' or 'crosslinked' situation. Interactions between the cosolutes, e.g., packing effects, are neglected. These effects have been included in a more complete calculation within a similar model previously.[38]

In case 1) the proximity of the plates increases the accessible volume for the cosolutes. The latter gain configurational entropy proportional to the freed volume $A\sigma$. This leads to a favorable (grand canonical) free energy per area

$$\Omega_1^*/A = -\sigma\rho_c^0 \qquad (5)$$

for $d < \sigma$. That is the well-known effective surface at-

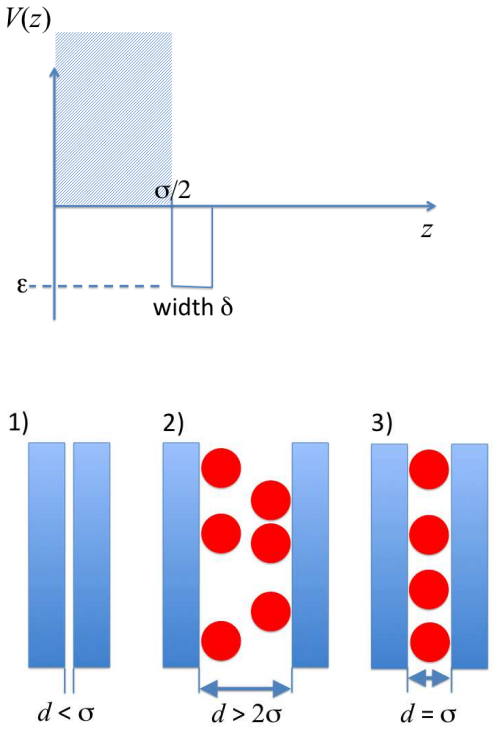

FIG. 5: Top: Generic interaction potential $V(z)$ between one cosolute and one plate-like monomer in a center-of-mass to surface distance z as assumed in our statistical mechanics approach. $\sigma/2$ is the cosolute hard-core radius, while $\epsilon < 0$ is the attractive well depth and δ is its width. Bottom: sketch of the three interaction situations of the simplified plate-like monomers (blue plates) in presence of the cosolutes (red spheres).

traction by particle depletion.[40] The grand canonical free energies for situations 2) and 3) can be explicitly written down and are

$$\Omega_2 = N_b \left[\ln\left(\frac{N_b\Lambda^3}{2A\delta}\right) - 1 \right] + N_b(\epsilon - \mu) \qquad (6)$$

and

$$\Omega_3 = N_b \left[\ln\left(\frac{N_b\Lambda^3}{A\delta}\right) - 1 \right] + N_b(2\epsilon - \mu), \qquad (7)$$

respectively, where Λ is the thermal wavelength, μ the chemical potential, and N_b is the number of bound particles. Note the difference between (2) and (3): In case 2), a particle gains energy ϵ by binding to one surface, but 2 surfaces, that is, twice the configuration space as in 3) is available in total (hence the factor 2 before A in the log-term). In situation 3), one particle gains 2ϵ by binding to two surfaces simultaneously, but effectively only one plane for the cosolute translation is available. The energies are minimized by the Boltzmann equations $N/(2\delta A) = \rho_c^0 \exp(-\epsilon)$ and $N/(\delta A) = \rho_c^0 \exp(-2\epsilon)$, respectively, where we used $\rho_c^0 = \Lambda^{-3}\exp(\mu)$. Plugging the solution back in (1) and (2) we obtain the minimum free energies per area

$$\Omega_2^*/A = -2\delta\rho_c^0 \exp(-\epsilon) \qquad (8)$$

and

$$\Omega_3^*/A = -\delta\rho_c^0 \exp(-2\epsilon). \qquad (9)$$

Inspection of the results shows that for very small $|\epsilon|$ situation 1) is favored over 2), that is, the depletion interaction wins. For increasing ϵ, however, situation 2) is favored over 1); when comparing $\Omega_1^* = \Omega_2^*$ we find $\epsilon_{12}^* = -\ln\sigma/(2\delta)$ which depends on the interaction range δ. For a LJ interaction, as in our simulation model, the width of the minimum roughly $\delta \simeq \sigma/3$ which yields $\epsilon_{12}^* \simeq -0.4$ for the crossover from depletion attraction to full solvation of the two monomers. Since the minimum free energies of the two situations 1) and 3), where $d \lesssim \sigma$, are both higher, this implies repulsion between close monomers. In colloidal physics this effect was coined 'repulsion through attraction'.[41,42] The free energy for situation 3), where bridging is favored, decreases faster with ϵ than in situation 2), because of the 2 in the exponent. By equating (8) and (9), we obtain the crossover energy $\epsilon_{23}^* = -\ln 2 \simeq -0.7$. For high attraction consequently situation 3) is favored.

Thus, we can now generally identify three regimes depending on the attractive interaction strength ϵ: i) $|\epsilon| \lesssim 0.4$: depletion attraction between surfaces (favoring collapse); ii) $0.4 \lesssim |\epsilon| \lesssim 0.7$: repulsion through attraction (favoring swelling); $|\epsilon| \gtrsim 0.7$: polymer-polymer attraction by bridging (favoring collapse). The situation is summarized in the 'phase diagram' in Fig. 6 for the specific value of $\delta = \sigma/3$. Note, however, that the attraction width plays a nontrivial role: if the attraction range is small compared to the cosolute size, $\delta < \sigma/4$, then $|\epsilon_{12}^*| > 0.7$, and situation 2) becomes metastable. In contrast, if δ is not small, $\delta \geq \sigma/2$, situation 2 is favored over 1) for any value $\epsilon > 0$ and the depletion scenario 1) becomes metastable. However, for a large attraction width, $\delta > \sigma/2$, the bridging case is ill-defined and is possibly indistinguishable anymore from the solvated case 2). We note that equivalent scenarios apply in mixtures of colloids and nanoparticles.[42,43]

The findings above may be important to understand controversial effects observed in experimental LCST measurements of polymers and simple peptides. Only if polymer-cosolute attractions are weak and not too short-ranged, swelling effects should be observable. This may be indeed valid for weak hydrophobic or dispersion attractions. In computer simulations in fact urea swells purely hydrophobic polymers.[20,44] In hydrogen bonding systems, however, the attraction length is short $\simeq 0.1 - 0.2$ nm and no swelling is possible. Consistent with that view, urea collapsed PNIPAM polymers which has been argued is due bridging by short-ranged

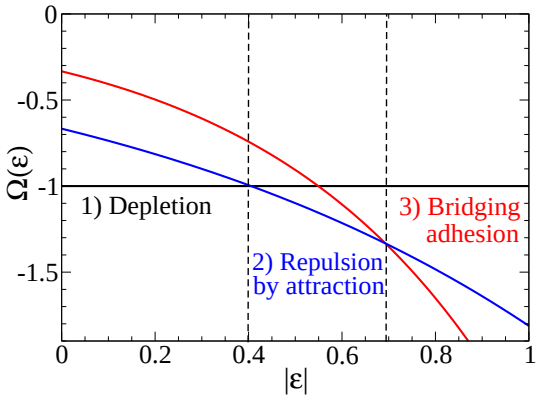

FIG. 6: Free energy branches for the situations 1)-3) depicted in Fig. 5 versus the cosolute-monomer interaction energy ϵ. Parameters chosen here are density $\sigma^3\rho_c^0 = 1$ and interaction width $\delta = \sigma/3$.

H-bonds, strongly supported by experimental means.[19] The same experiments also showed urea-induced swelling of hydrophobic peptides. Consistent with our picture it was argued that this is due to much weaker, not short-ranged attractions.[19]

Looking at the quantitative numbers predicted by the present theory they are surprisingly close to the ones observed in our simulations. The chain was found to be most swollen in the weakly attractive regime $\epsilon \simeq 0.3 - 0.6$ for not too high values of intrapolymer attraction. Thus although highly simplified, the effective one-component approach seems to capture most of the underlying physics.

IV. TWO-COMPONENT FLORY - DE GENNES MODEL

Another perspective to polymer collapse in a highly attractive cosolute dispersion could be based on a mean-field Flory-de Gennes picture where all interactions are described by 2nd and 3rd order virial coefficients. In contrast to an effective one-component model as typically used in literature, cf. eq. (1), we now investigate the full two-component description.

Consider a polymer with N monomers and an effective bond length b in contact with a reservoir of cosolutes with density ρ_c^0. As usual in Flory theory we take now the end-to-end distance R to represent the size of the polymer coil. In this view the monomer density profile is just a step function with a constant monomer number density $\rho_m = N/V = 3N/(4\pi R^3)$ inside the coil with volume V. In the spirit of mean-field Flory theory for real chains the excess free energy due to interactions can be expressed in terms of the virial expansion in the monomer density ρ_m and the cosolute density ρ_c within the coil. A Flory-like free energy of the system can be then written as

$$F(R) = \frac{3R^2}{2Nb^2} + \frac{\pi^2 Nb^2}{12R^2} + V\sum_{ij=m,c}\rho_i\rho_j B_2^{ij} + \frac{V}{2}\sum_{ijk=m,c}\rho_i\rho_j\rho_k B_3^{ijk}, \quad (10)$$

where the first term denotes the elastic free energy of the ideal chain, the second term is a correction due to confinement entropy for highly collapsed states,[3,45] and the last two terms are the virial corrections up to third order. The density $\rho_c = \rho_c(R)$ denotes the cosolute density inside the polymer which is related to the bulk concentration ρ_c^0 by

$$\rho_c(R) = \rho_c^0 \exp(-\mu_{\rm exc}) \quad (11)$$

with the the excess chemical potential

$$\mu_{\rm exc} = \frac{\partial}{\partial\rho_c}\left[\sum_{ij=m,c}\rho_i\rho_j B_2^{ij} + \frac{1}{2}\sum_{ijk=m,c}\rho_i\rho_j\rho_k B_3^{ijk}\right]_V \quad (12)$$

The coupled eqs. (10) to (12) provide a free energy expression as a function of R, the polymer size for given interactions V_{ij}, with $i = c, m$, as provided by eq. (2), polymerization N, bond length b, and cosolute concentration ρ_c^0. To obtain the equilibrium radius R and corresponding monomer and cosolute densities we minimize (10) according to $\partial F/\partial R = 0$ numerically using an iterative Newton-Raphson scheme. Due to the relative simplicity of the equations this takes only seconds on a single, ordinary computing processor.

The B_2 values are explicitly calculated using definition (4). To connect properly to our computer simulation, where $\epsilon_{cc} = 0.3$ and thus B_2^{cc} vanishes, we set $B_2^{cc} = 0$ accordingly. We have also explicitly calculated all values B_3^{ijk} but found that they can be well approximated by a constant $B_3^{ijk} = 2\sigma^6$. The latter actually closely corresponds to the 3rd virial coefficient of hard spheres with diameter σ. In other words the B_3 values reflect mostly packing effects by hard spheres with size σ.

Results for the polymer size $R(\epsilon_{mc})$ are plotted in Fig. 7 as a function of ϵ_{mc} for $\epsilon_{mm} = 0.2$, 0.3, 0.4, and 0.6 (cf. curves in Fig. 2). The radius is scaled by $R_0 = 3.27$ nm which is the ideal chain size according to the Flory approach. As in the simulation the chain is collapsed for small ϵ_{mc} due the addition of repulsive cosolutes. Increasing ϵ_{mc} leads to chain swelling up to a maximum coil size with a corresponding ϵ_{mc}^{max} that increases with ϵ_{mm}. This trend reproduces the one found in the simulation. Further increase of ϵ_{mc} leads to deswelling and reentrant collapse. For the three smaller values of ϵ_{mm} the collapse transition is at about $\epsilon \simeq 0.7$. This value is interestingly in agreement with the value obtained in the effective one-component approach for the crossover from swelling to collapse. This may be accidental. However, all three approaches show the same

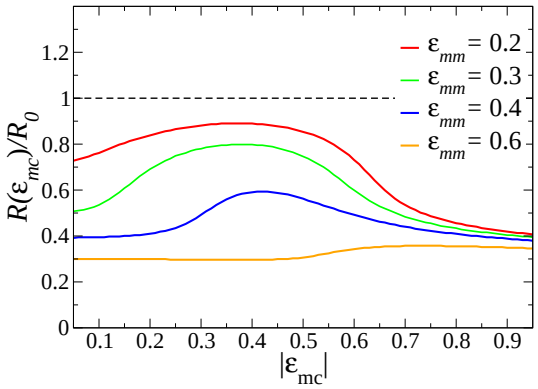

FIG. 7: The polymer radius R scaled by its ideal value R_0 from minimization of the two-component Flory-de Gennes free energy eq. (10) versus polymer-cosolute interaction strength ϵ_{mc}. The plot is for a polymer-polymer interaction ϵ = 0.2, 0.3, 0.4, and 0.6 . The polymer shows transitions from collapsed states to swollen and collapsed states again , in qualitative agreement with the Langevin computer simulations (cf. Fig. 2).

qualitative features and numbers in the same ballpark. Importantly, also the two-component Flory describes the reentrant collapse in strongly attractive cosolute conditions. Note that the mean-field theory does not provide 'swelling' as defined by $R/R_0 > 1$.Trends, however, are, as discussed above, nicely in accord.

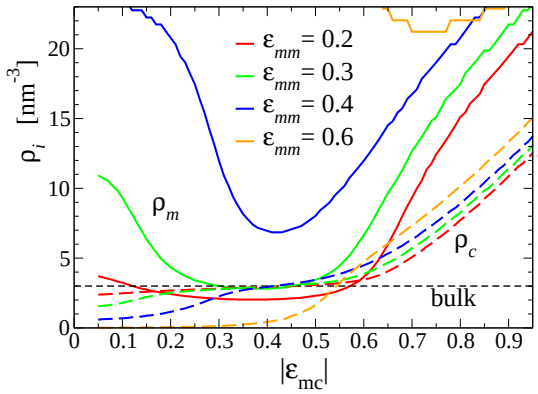

FIG. 8: The mean monomer density ρ_m (solid lines) and cosolute density ρ_c (dashed line) inside the polymer coil versus monomer-cosolute attraction ϵ_{mc} and varying ϵ_{mm} = 0.2, 0.3, 0.4, and 0.6 (see legend). The curves are from the solution of the two-component Flory-like model for polymer collapse and swelling. For the three smaller ϵ_{mm} values, at the minimum of ρ_m the cosolute density ρ_c is comparable to its bulk value (horizontal dashed black line).

The mean monomer and cosolute densities $\rho_m(\epsilon_{mc})$ and $\rho_c(\epsilon_{mc})$, respectively, are plotted in Fig. 8 for ϵ_{mm} = 0.2, 0.3, 0.4, and 0.6 as a function of ϵ_{mc}. The monomer density ρ_m decreases and increases according to the swelling behavior $\rho_m \propto R^{-3}$ (cf. Fig. 7). The mean cosolute density ρ_c monotonically increases with ϵ_{mc}. For small values $\epsilon_{mc} < 0.4$, cosolutes are depleted from the polymer coil due to repulsive interactions. At $\epsilon_{mc} = 0.4$, the density goes down to one third of the bulk density, comparable to the decrease found in the simulations, cf. Fig. 4. For the three smaller values of ϵ_{mm} at around ϵ_{mc} = 0.4, where the polymer is most swollen, there is a plateau in the mean density which almost exactly corresponds to bulk density. Remarkably this reproduces the observation in the simulation profiles in Fig. 4, where we found a homogenous bulk-like density in the most swollen state of the coil. For the largest plotted $\epsilon_{mm} = 0.6$ where polymer compaction is very strong this correspondence between the minimum in ρ_m and plateau ρ_c is lost for whatever reason. For further increasing $\epsilon_{mc} \gtrsim 0.5$ the cosolute density ρ_c within the polymer further grows for all values of ϵ_{mm} while the chain is collapsing again. Thus, consistent with the simulations, chain collapse driven by highly attractive polymer-cosolute interactions leads to highly dense cosolute states inside the coil. The density of about 14 nm^{-3} is about twice as high as in the simulation, cf. Fig. 4, but the Flory prediction of one-order-of-magnitude increase inside the globule is qualitatively correct.

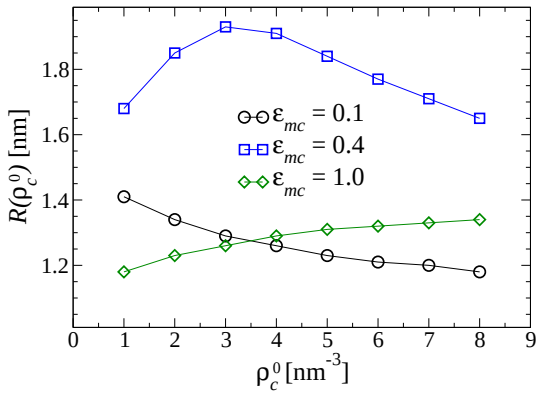

FIG. 9: Polymer size $R(\rho_c^0)$ in dependence of cosolute bulk density ρ_c^0 from the two-component Flory-like approach. Data are for a fixed monomer-monomer attraction ϵ_{mm} = 0.4 and varying monomer-cosolute attractions ϵ_{mc} = 0.1, 0.4, and 1.0. Note that only the case ϵ_{mc} = 0.4 exhibits nonmonotonic behavior.

Finally, we can use the Flory-like approach to make predictions about the dependence of polymer size R on the cosolute density reservoir (or bulk) density ρ_c^0. The calculated $R(\rho_c^0)$ is plotted in Fig. 9 in dependence of cosolute bulk density ρ_c^0 for a fixed monomer-monomer attraction ϵ_{mm} = 0.4 and varying monomer-cosolute at-

tractions $\epsilon_{mc} = 0.1$, 0.4, and 1.0. The density range covers typical denaturant concentration from 1 to 8 nm^{-3}, that is, 1.7 to 13.3 mol/l. In the case $\epsilon_{mc} = 0.1$, R decreases monotonically with density. This is expected for a depletion-like collapse mechanism, where the effect grows with density. In contrast, in the case $\epsilon_{mc} = 1.0$, R *increases* monotonically with density. That indicates that the collapse effect due to highly attractive cosolute deteriorates with increasing cosolute density. Remarkably, for $\epsilon_{mc} = 0.4$, where swelling is found for weakly attractive cosolutes, the size behavior is *nonmonotonic.* This is interesting in the light of LCST measurements of poly(NIPAM) and elastin-like peptides in Hofmeister salts.[18,27] Nonmonotonic behavior of the LCST change with salt concentration was indeed observed only in the swelling scenarios. This happened for the salts NaI and NaSCN which seem to feature weakly attractive interactions with nonpolar peptide groups.[28]

V. SUMMARY AND CONCLUDING REMARKS

The coarse-grained computer simulations performed here and elsewhere[26] demonstrate polymer collapse to compact globular states at highly attractive cosolute conditions. The polymer response and relative swelling/collapse behavior is most pronounced for polymers in nearly ideal Θ-like solvent conditions. Here the polymer can shrink or swell considerably, depending on polymer-monomer interaction strength. Collapsed states for repulsive and strongly attractive cosolutes are physically different as in the latter state the polymer coil is rich in cosolutes. For the same polymer size the internal cosolute density can differ enormously between 1/2 to 1/3 of the bulk density (repulsive cosolutes) and 8 times the bulk density (highly attractive case), respectively, signifying considerably different physical properties of the globule-cosolute system. The most swollen polymer state is characterized by a bulk like cosolute density inside the polymer coil.

We further demonstrate that the transition to collapsed states in strongly attractive cosolutes can be rationalized by two independent theoretical and semi-analytical approaches. Their implications are summarized in the following.

The 'effective one-component statistical mechanics model' showed that for large polymer cosolute attraction bridging interactions (leading to compact 'glued' states) are energetically favored over both depletion interaction (favoring collapse by exclusion) and 'repulsion by attraction' situation (leading to swelling). We have shown that a critical parameter to distinguish those scenarios is the ratio between interaction width and cosolute size δ/σ. Only if polymer-cosolute interactions are not too short-ranged swelling effects should be observable. This may be valid for hydrophobic or dispersion attractions. In simulations indeed urea swells purely hydrophobic polymers[20,44] or hydrophobic peptides.[19] In hydrogen bonding systems, however, the attraction length is short $\delta/\sigma \simeq 1/4$ or 1/5 and no swelling is possible. Consistent with that view, urea compresses PNIPAM polymers which has been argued is due to H-bonding and crosslinking by bivalent binding as demonstrated by experiments.[19] Methylated urea did not swell PNIPAM, neither did urea swell elastin-like peptides.

The two-component Flory-de Gennes mean-field model also predicts polymer collapse at strongly attractive cosolute conditions. The transition from swollen to collapsed state at a polymer-cosolute attraction energy of $-\ln 2\ k_B T$ is in good agreement with our computer simulations and the effective one-component approach. In particular, the Flory model confirmed that cosolute densities inside the coil can significantly differ between repulsive cosolutes and strongly attractive ones. It also reproduced the simulation finding that the polymer is most swollen if internal cosolute density exactly matches bulk density for nearly ideal cosolutes. Thus, the structural nature of collapsed states can be qualitatively different while the polymeric state alone, on a first glance, may be similar. The Flory approach also predicts a nonmonotonic dependence of swelling magnitude with cosolute density, which is observed for PNIPAM or elastin in NaI and NaSCN.[18,27] A more detailed investigation may shed more light on the reason why.

We note that dense cosolutes in polymer coils may have strong impact on internal friction and viscosity of polymeric globules. Consequently, the conformational kinetics of polymers maybe highly affected by explicit direct-binding cosolutes in contrast to isolated polymers.[37]

Our findings may have implications on the interpretation of denaturant action on proteins and the nature of denatured states. For instance, the structure of molten globular proteins denatured by high $NaClO_4$ (sodium perchlorate) is controversially discussed.[5,29,30] Considering our results and the experimentally known strong affinity of $NaClO_4$ to the protein backbone,[10,11,28] the reason for the difficulties may be a large amount of bridging or crosslinking denaturant which probably strongly obscures the experimental characterization of structure and its classification.

Finally, similar considerations as above may be important in the interpretation of ion-induced collapse of polyelectrolytes beyond simple electrostatics.[33–36]

Acknowledgments

A.M. thanks the European Erasmus Programme for financial support. J.H. and J.D. acknowledge funding from the Alexander-von-Humboldt Stiftung, Germany.

* To whom correspondence should be addressed. E-mail: joachim.dzubiella@helmholtz-berlin.de

[1] P. J. Flory, *Principles of Polymer Chemistry* (Cornell University Press, Ithaca, 1953).
[2] P. G. de Gennes, *Scaling Concepts in Polymer Physics* (Cornell University Press, Ithaca, 1979).
[3] M. Rubinstein and R. Colby, *Polymer Physics* (Oxford University Press, New York, 2003).
[4] B. M. Baysal and F. E. Karasz, Macromol. Theory Simul. **12**, 627 (2003).
[5] J. M. Scholtz and R. Baldwin, Biochemistry **32**, 4604 (1993).
[6] B. Bennion and V. Daggett, Proc. Natl. Acad. Sci (USA) **100**, 5142 (2003).
[7] M. Auton and D. W. Bolen, Proc. Natl. Acad. Sci (USA) **102**, 15065 (2005).
[8] E.P.O'Brien, G. Z. G. Haran, and B. R. B. D. Thirumalai, Proc. Natl. Acad. Sci (USA) **105**, 13403 (2008).
[9] Y. Zhang and P. S. Cremer, Annu. Phys. Rev. Chem. **61**, 63 (2010).
[10] L. M. Pegram, T. Wendorff, R. Erdmann, I. Shkel, D. Bellissimo, D. J. Felitsky, and M. T. Record, Proc. Natl. Acad. Sci. **107**, 7716 (2010).
[11] E. J. Guinn, L. M. Pegram, M. W. Capp, M. N. Pollock, and M. T. Record, Proc. Natl. Acad. Sci. **108**, 16932 (2011).
[12] D. R. Canchi, D. Paschek, and A. E. Garcia, J. Am. Chem. Soc. **132**, 2338 (2012).
[13] D. R. Canchi and A. E. Garcia, Biophys. J. **100**, 1526 (2011).
[14] C. E. Dempsey, P. E. Mason, and P. Jungwirth, J. Am. Chem. Soc. **2011**, 73007303 (133).
[15] J. Heyda, M. Kozisek, L. Bednárova, G. Thompson, J. Konvalinka, J. Vondrásek, and P. Jungwirth, J. Phys. Chem. B **115**, 89108924 (2011).
[16] K. Dill, S. Bromberg, K. Yue, K. Fiebig, D. Yee, P. Thomas, and H. Chan, Protein Sci. **4**, 561 (1995).
[17] H. Chan and K. Dill, Annu Rev Biophys Bio **20**, 447 (1991).
[18] Y. Zhang, S. Furyk, D. Bergbreiter, and P. Cremer, J. Am. Chem. Soc. **127**, 14505 (2005).
[19] L. B. Sagle, Y. Zhang, V. A. Lithosh, X. Chen, Y. Cho, and P. S. Cremer, J. Am. Chem. Soc. **131**, 9304 (2009).
[20] R. Zangi, R. Zhou, and B. J. Berne, J. Am. Chem. Soc. **131**, 1535 (2009).
[21] T. Ghosh, A. Kalra, and S. Garde, J. Phys. Chem. B **109**, 642 (2005).
[22] M. V. Athawale, S. Sarupria, and S. Garde, J. Phys. Chem. B **112**, 5661 (2008).
[23] R. Godawat, S. N. Jamadagni, and S. Garde, J. Phys. Chem. B **2010**, 2246 (114).
[24] J. M. Polson and N. E. Moore, J. Chem. Phys. **122**, 024905 (2005).
[25] C. P. Lowe and M. W. Dreischor, J. Chem. Phys. **122**, 084905 (2005).
[26] D. Antypov and J. A. Elliott, J. Chem. Phys. **129**, 174901 (2008).
[27] Y. Cho, Y. Zhang, T. Christensen, L. B. Sagle, A. Chilkotia, and P. S. Cremer, J. Phys. Chem. B **112**, 13765 (2008).
[28] L. M. Pegram and M. T. Record, J. Phys. Chem. B **112**, 9428 (2008).
[29] A. H. Crevenna, N. Naredi-Rainer, D. C. Lamb, R. Wedlich-Söldner, and J. Dzubiella, Biophys. J. **102**, 907 (2012).
[30] D. Hamada, Proc. Natl. Acad. Sci. **91**, 10325 (1994).
[31] G. Haran, Curr. Opin. Struct. Biol. **22**, 14 (202).
[32] R. L. Baldwin, C. Frieden, and G. Rose, Proteins **78**, 2725 (2010).
[33] R. G. Winkler, M. Gold, and P. Reineker, Phys. Rev. Lett. **80**, 3731 (1998).
[34] A. R. Khokhlov and E. Y. Kramarenko, Macromolecules **29**, 681 (1996).
[35] H. Schiessel and P. Pincus, Macromolecules **31**, 7953 (1998).
[36] M. Muthukumar, J. Chem. Phys. **120**, 9343 (2004).
[37] N. M. Toan, G. Morrison, C. Hyeon, and D. Thirumalai, J. Phys. Chem. B **112**, 6094 (2008).
[38] B. Rózicky, R. Lipowsky, and T. R. Weikl, Europhys. Lett. **84**, 26004 (2008).
[39] D. V. D. Spoel, E. Lindahl, B. Hess, G. Groenhof, A. E. Mark, and H. J. C. Berendsen, Comp. Chem. **26**, 1701 (2005).
[40] R. J. Hunter, *Foundations of Colloid Science* (Oxford University Press, Oxford, 2001).
[41] A. A. Louis, E. Allahyarov, H. Löwen, , and R. Roth, Phys. Rev. E **65**, 061407 (2002).
[42] S. Karanikas and A. A. Louis, Phys. Rev. Lett. **93**, 248303 (2004).
[43] E. N. Scheer and K. S. Schweizer, J. Chem. Phys. **128**, 164905 (2008).
[44] M. Lee and N. F. A. van der Vegt, J. Am. Chem. Soc. **128**, 4948 (2006).
[45] M. Doi and S. F. Edwards, *The Theory of Polymer Dynamics* (Clarendon Press, Oxford, 1986).